HHS Public Access

Author manuscript

Birth Defects Res. Author manuscript; available in PMC 2024 November 15.

Published in final edited form as:

Birth Defects Res. 2023 November 15; 115(19): 1851–1865. doi:10.1002/bdr2.2216.

Ezh2-dependent methylation in oral epithelia promotes secondary palatogenesis

Bo Sun[#],

Kurt Reynolds[#],

Subbroto Kuma Saha,

Shuwen Zhang,

Moira McMahon,

Chengji J Zhou[*]

Institute for Pediatric Regenerative Medicine of Shriners Hospital for Children – Northern California & Department of Biochemistry and Molecular Medicine, School of Medicine, University of California at Davis, Sacramento, CA 95817, USA

Abstract

Background: In addition to genomic risk variants and environmental influences, increasing evidence suggests epigenetic modifications are important for orofacial development and their alterations can contribute to orofacial clefts. Ezh2 encodes a core catalytic component of the Polycomb repressive complex responsible for addition of methyl marks to Histone H3 as a mechanism of repressing target genes. The role of Ezh2 in orofacial clefts remains unknown.

Aims: To investigate the epithelial role of Ezh2-dependent methylation in secondary palatogenesis.

Methods: We used conditional gene-targeting methods to ablate Ezh2 in the surface ectoderm-derived oral epithelium of mouse embryos. We then performed single-cell RNA sequencing combined with immunofluorescence and RT-qPCR to investigate gene expression in conditional mutant palate. We also employed double knockout analyses of Ezh1 and Ezh2 to address if they have synergistic roles in palatogenesis.

Results: We found that conditional inactivation of Ezh2 in oral epithelia results in partially penetrant cleft palate. Double knockout analyses revealed that another family member Ezh1 is dispensable in orofacial development, and it does not have synergistic roles with Ezh2 in palatogenesis. Histochemistry and single-cell RNA-seq analyses revealed dysregulation of cell cycle regulators in the palatal epithelia of Ezh2 mutant mouse embryos disrupts palatogenesis.

Conclusion: Ezh2-dependent histone H3K27 methylation represses expression of cell cycle regulator Cdkn1a and promotes proliferation in the epithelium of the developing palatal shelves. Loss of this regulation may perturb movement of the palatal shelves, causing a delay in palate elevation which may result in failure of the secondary palate to close altogether.

[*]**Correspondence author:** cjzhou@ucdavis.edu.
[#]Bo Sun and Kurt Reynolds contributed equally to this study.

Conflicts of interests. Authors declare no conflicts of Interests.

Keywords

Cleft palate; Ezh2; H3K27me3; methylation; scRNA-seq; orofacial epithelia; proliferation

1 INTRODUCTION

Orofacial cleft (OFC) is one of the most common birth defects, impacting 1 in 700 newborns globally (Watkins et al., 2014). The most common types are cleft lip with or without cleft palate (CL/P) and cleft palate only (CPO). Each year, around 2,650 babies are born with CPO in the United States, and 4,440 babies have a CLP (according to NIH report, July 2018). The affected children experience significant difficulties in feeding, language development and social integration. Although plastic and maxillofacial surgery, speech therapy and psychosocial intervention are available, OFC is associated with significant long-term health, life-style wellbeing and socio-economic burdens for individuals and their families (Dixon et al., 2011).

All mammalian species go through a similar palatogenesis process. In humans, the development of the secondary palate begins from the end of the sixth week of embryonic development and is completed in the ninth week, as a consequence of an intact palate is formed (Burdi and Faist, 1967). In mice, the secondary palate develops as an outgrowth of the maxillary prominences at about embryonic day 11.5 (E11.5); the palatal shelves grow vertically (E12.5 and E13.5) and then subsequently elevated on both sides of the tongue at E14.5 (Bush and Jiang, 2012; Ji et al., 2020). Once the palatal shelves have elevated to a horizontal position above the tongue, they will continue to converge toward the midline and adhere with each other. The transient midline epithelial seam (MES) is formed at around E15 which will be eliminated after the fusions of two palatal shelves at around E15.5 when the palatogenesis is completed (Bush and Jiang, 2012). Several processes may contribute to MES dissolution, including epithelial-to-mesenchymal transition, outward cell migration, apoptosis, convergence and extrusion (Carette and Ferguson, 1992; Cuervo et al., 2002; Jin and Ding, 2006; Kim et al., 2015; Mori et al., 1994; Shuler et al., 1992). A more recent study using novel static- and live-imaging approaches reveals that the MES is removed through streaming migration of epithelial cells during palatal fusion (Teng et al., 2022). Disruptions at any stages may cause cleft palate, including submucous cleft if fusion is incomplete.

Genome-wide association studies over the past couple decades have identified at least 40 candidate genes and loci whose polymorphisms are associated with OFC risk (Beaty et al., 2011, 2010; Birnbaum et al., 2009; Butali et al., 2013; Elizabeth J. Leslie et al., 2016; Elizabeth J Leslie et al., 2016; Leslie et al., 2017, 2015; Ludwig et al., 2016, 2012; Marazita et al., 2009, 2004; Moreno et al., 2009; Mukhopadhyay et al., 2022, 2021; Reynolds et al., 2020; Sun et al., 2015; van Rooij et al., 2019; Yu et al., 2017). Epigenomes (e.g., DNA methylation and histone modification) influenced by the environment regulate chromatin structure and genome functions. It is also well established that environmental factors affecting OFC incidence, such as diet, behavior, and disease, are important regulators of epigenetic modifications (Campos Neves et al., 2016; Czeizel et al., 1999; Garland et al.,

2020a; Spilson et al., 2001). It is, therefore, highly likely that aberrant epigenetic control of gene expression in response to environmental risk factors also plays a major role in the etiology of OFC.

There is increasing data demonstrating that alterations in epigenetic modifications affecting gene expression may contribute to the etiology of OFC (Garland et al., 2020b; Seelan et al., 2012). It has been understood for some time that administration of the DNA demethylating agent 5-aza-2′-deoxycytidine can induce cleft palate in both mice and rats (Branch et al., 1999; Bulut et al., 1999; Rogers et al., 1994). Additionally, the palatal tissue of mouse embryos with retinoic acid-induced cleft palate shows significantly elevated DNA methylation in both CpG islands and gene bodies of known palatogenesis regulators (Kuriyama et al., 2008; Shu et al., 2018). Similarly, altered methylation at several loci with genome-wide OFC association has been demonstrated in lip and palate tissue of NSCL/P patients as well (Alvizi et al., 2017; Gonseth et al., 2019; Howe et al., 2019; Z. Xu et al., 2019).

In addition to DNA methylation, histone modifications are also important for craniofacial development and alterations contribute to OFC and related craniofacial birth defects. Histone acetyltransferase activity and H3 acetylation is increased in the palatal tissue of mouse embryos with 2,3,7,8-tetrachlo-rodibenzo-p-dioxin-induced cleft palate (Yuan et al., 2016). Several enzymes that regulate histone acetylation play roles in OFCs as well. For example, mutations in the mouse H3 acetyltransferase gene *Kat6b* cause a 22q11 deletion-like phenotype including cleft palate (Voss et al., 2012). Alternatively, conditional loss of function of the histone deacetylase gene *Hdac3* in neural crest cells also causes craniofacial abnormalities with fully penetrant cleft palate (Singh et al., 2013).

Histone methylation is another mechanism understood to play important roles in gene regulation with implications in palate development. *Prdm3* and *Prdm16* comprise a subfamily of two closely related genes encoding enzymes with histone methyltransferase activity at that at H3K4 and H3K9. Loss of *Prdm16* function in mice causes cleft palate (Bjork et al., 2010). While loss of *Prdm3* is lethal during mid-gestation, conditional *Prdm16* knockout in *Sox2*-expressing cells causes partially penetrant cleft palate with significantly decreased H3K9 methylation in the palatal shelves, which is associated with gene repression. Interestingly, H3K4 methylation, which contributes to gene activation, was unaltered (Shull et al., 2020). Two other enzymes that methylate H3K4 are KDM6A and KTM2D. Mutations in either *KMD6A* or *KTM2D* can causes Kabuki syndrome, which is typified by facial characteristics that include midfacial hypoplasia with a broad depressed nasal tip, elongated palpebral fissures with partial eyelid eversion, and abnormally prominent earlobes, with partially penetrant cleft palate (Hannibal et al., 2011; Lindgren et al., 2013). Additionally, targeting *Kmd6a* in mouse neural crest using *Wnt1-Cre* causes Kabuki-like features in females including 25% cleft palate, targeting Ktm2d causes fully penetrant cleft palate. However, alterations in histone methylation were not identified, suggesting alternate mechanisms may contribute to facial defects (Shpargel et al., 2020, 2017). Despite these recent advancements, little is known about the role that H3K27 methylation, one of the major histone modifications that controls gene expression, plays in craniofacial and palate development. Even though no link was identified in mouse models,

the previously discussed *Kmd6a* possesses H3K27 demethylase capabilities in addition to its role in methylating H3K4 (Lindgren et al., 2013).

Enhancer of zeste homolog 2 (*Ezh2*) encodes a critical factor of epigenetic modification and is an essential regulator of cell proliferation and differentiation during mammalian embryonic development (Aloia et al., 2013; Huang et al., 2014; O'Carroll et al., 2001). EZH2 is a key component of Polycomb Repressive Complex 2 as primary enzyme responsible for catalyzing di- and tri-methylation to histone H3 at K27 (Kuzmichev et al., 2002; Müller et al., 2002). *Ezh2* is necessary for development of neural crest-derived cartilage and bone, and ablation of *Ezh2* in murine neural crest cells causes severe craniofacial defects including absence of tongue and mandible, microtia and microphthalmia, and meningoencephalocele (Kim et al., 2018; Schwarz et al., 2014). Additionally, *Ezh2* controls proliferation in the dental mesenchyme by regulating the cell cycle inhibitor *Cdkn2a*, expression of which is increased in *Ezh2* mutants (Jing et al., 2019). While a relationship has not been demonstrated in oral tissues, *Ezh2* can also repress expression of *Cdkn1a*, which encodes key cell cycle regulator p21 with implications in several cancers (Béguelin et al., 2017; Fan et al., 2011; J. Xu et al., 2019).

Epigenetic modification is time- and tissue-specific, and allows individual cell types respond differently to the same stimulus (John and Rougeulle, 2018; Kanherkar et al., 2014). It is, therefore, a challenge to dissect the specific roles of epigenetic modification in disease development. Single-cell RNA-sequencing (scRNA-seq) provides an advanced tool to study differences in gene expression at a single-cell resolution (Stuart et al., 2019). Using a Cre-lox approach, we demonstrated that conditional knockout (cKO) of *Ezh2* in oral epithelial cells causes partial penetrant CPO in mice, with absent H3K27 trimethylation and reduced proliferation in the palate epithelium. Further, *Ezh1* in the oral epithelium is dispensable and has no synergetic roles with Ezh2 for secondary palatogenesis. Using scRNA-seq, we identified significant differential expression of transcriptomes of cell cycle regulators in the epithelial populations of the mutant mouse palate relative to control littermates prior to palatal fusion at the midline.

2 MATERIALS AND METHODS

2.1 Animals

The Grhl3^{Cre} knock-in mouse line (Camerer et al., 2010) was acquired through the Mutant Mouse Resource & Research Centers (MMRRC) at UC Davis. Ezh1-null (Ezhkova et al., 2011) and Ezh2-flox (Shen et al., 2008) mice were obtained from Dr. Elena Ezhkova at Icahn School of Medicine at Mount Sinai, and Rosa26-mT/mG (Muzumdar et al., 2007) mice from the Jackson Laboratory. Heterozygous or homozygous alleles were maintained against a C57BL/6J background. Pregnant, timed-mated mice were anesthetized with isoflurane before being sacrificed by cervical dislocation for embryo dissection and collection. Mice were housed at the UC Davis Vivarium with a standard 12-hour light/dark cycle and all animal procedures were performed in accordance with IACUC and NIH guidelines.

2.2 Hematoxylin and eosin staining

Embryos were drop-fixed in 4% PFA overnight, dehydrated, embedded in paraffin (Sigma Paraplast P3558), and sectioned at 6 μm. Sections were rehydrated, submerged in Gill's Hematoxylin (Sigma GHS232) 20 minutes, and excess stain washed briefly with 1% acid alcohol. Li2CO3 was used for bluing before submerging sections in eosin Y solution (Sigma HT110216) for 15 minutes. Sections were then dehydrated and mounted for imaging.

2.3 Immunofluorescent labeling

Embryos were drop-fixed in 4% PFA, embedded in OCT after 30% sucrose cryoprotectant equilibration overnight, and sectioned at 12 μm. Sections post-fixed in 4% PFA and heated at low boil in Sodium Citrate buffer pH = 6.0 for antigen retrieval. Sections were washed 5 minutes in 0.1% Triton X-100 for improved permeation before 1 hr block in 10% Normal Donkey Serum. Antibodies used: rabbit anti-Ki67 1:200 (Abcam ab15580), rabbit anti-CASPASE 3 (cleaved) 1:200 (CST 9664S), mouse anti-E-Cadherin 1:200 (BD Bio 610181), rabbit anti-H3K37Me3 1:200 (CST 9733S). Tissues were counterstained with DAPI. Mesenchyme cells were quantified in ImageJ. Epithelial cells were counted manually. Two-tailed student's t-test was used for statistical comparison.

2.4 Single-cell RNA sequencing analyses

Palatal shelves were microdissected from *Grhl3*$^{Cre/+}$;*Ezh2*$^{flox/+}$ and *Grhl3*$^{Cre/+}$;*Ezh2*$^{flox/flox}$ mouse embryos on the morning of E14, prior to palatal convergence and epithelial fusion at the midline, and dissociated using a psychrophilic protease method (Adam et al., 2017). Dead cells were removed by FACS based on DAPI uptake in collaboration with the UC Davis Flow Cytometry Core, and live cells were processed with 10X Genomics 3' Chromium pipeline and Illumina (HiSeq4000)-sequenced in collaboration with the UC Davis DNA Technologies Core. Initial data was processed via Cell Ranger 7.0 (10X Genomics), reads mapped to the mm10 mouse genome, and samples subjected to quality control (Gu et al., 2022). Cells from each sample showing fewer than 800 or more than 15000 UMIs and those having less than 200 detected genes were discarded. Decontamination of ambient RNA was performed using decontX (Yang et al., 2020) model (github.com/campbio/celda), with this method producing 10,626 cells for *Grhl3*$^{Cre/+}$;*Ezh2*$^{flox/+}$ and 2,809 cells for *Grhl3*$^{Cre/+}$;*Ezh2*$^{flox/flox}$. Clustering and subclustering were determined through initial clustering of cells using the Seurat R toolkit combined with CellfindR (Satija et al., 2015; Yu et al., 2019) with clusters being annotated based on known cell type-specific genes. Cell-cell communications through ligand-receptor signaling interactions were analyzed by CellChat (Ji et al., 2020) and trajectory inference analysis was performed using *dynverse* (Cannoodt et al., 2021).

2.5 Total RNA isolation and RT-qPCR

Mouse embryonic palatal shelves from six Grhl3-Cre;Ezh2-cKO;Ezh1-KOs and six littermate controls at E14 were microdissected in RNase-free PBS for total RNA extraction using the RNeasy kit from QIAGEN. For RT-qPCR, we followed a previously established protocol with slight modifications (Gu et al., 2022). To synthesize cDNAs for subsequent qPCR analysis, we employed the iScript cDNA synthesis kit from Bio-

Rad, using 400 ng of total RNA per sample. The qPCR reactions were carried out in duplicate using the TB Green Advantage qPCR Premix by Takara Bio and the AriaMx real-time PCR system from Agilent Technologies. The ΔCT method was used to calculate the relative expression levels of the target genes, and the housekeeping gene Gapdh was used for result normalization. Mean ± S.D. values were determined, and statistical analysis (two-tailed, unpaired Student's t-test adjusted with Welch's correlation) was performed using GraphPad Prism V9.1 software. We applied a significance threshold of $P < 0.05$. The following primers were used in this study: *Cdkn1a*, 5'-*TTGCACTCTGGTGTCTGAG*-3' (forward) and 5'- *GTGATAGAAATCTGTCAGGCTG*-3' (reverse); *Cenpf*, 5'-*GCACAGCACAGTATGACCAGG*-3' and 5'-*CTCTGCGTTCTGTCGGTGAC*-3'; *Mki67*, 5'-*ATCATTGACCGCTCCTTTAGGT*-3' and 5'-*GCTCGCCTTGATGGTTCCT*-3'; *Top2a*, 5'-*CAACTGGAACATATACTGCTCCG*-3' and 5'- *GGGTCCCTTTGTTTGTTATCAGC*-3'.

3 RESULTS

3.1 Conditional ablation of *Ezh2* in oral ectoderm causes partial penetrant cleft palate

To target *Ezh2* in the palatal epithelium, we employed a knock-in Cre allele at *Grhl3* locus that activates at the surface ectoderm during embryonic development (Camerer et al., 2010). This line was crossed with conditional ready mice containing *loxP* sites at flanking the Set domain of *Ezh2*. This allele has no catalytic activity when recombined by active Cre leading to a loss of PRC2 function (Shen et al., 2008). We generated single and compound mutant embryos to assess phenotypic defects in the absence of functional polycomb complex activity. We crossed the $Grhl3^{Cre}$ line with *Rosa26-mTmG*, which contains a reporter allele in which tdTomato is constitutively expressed in all cells until Cre activation recombines eGFP in frame, after which all cells and progeny are labeled by eGFP expression (Muzumdar et al., 2007), allowing us to map the fate of $Grhl3^{+}$ cells in our model. The mTmG reporter tracing suggests $Grhl3^{Cre}$ efficiently activates in oral epithelium with sporadic clusters of GFP^{+} cells in the mesenchymal tissues (Figure 1a,b). Conditional ablation of Ezh2 with $Grhl3^{Cre}$ in the palatal epithelia abolished H3K27 trimethylation and caused partial penetrant cleft palate (Figure 1c–f).

Ezh1 is dispensable in the surface epithelium for craniofacial development, as no craniofacial defects or other obvious phenotypes found in *Ezh1-null* ($Ezh1^{-/-}$) mice that are viable and fertile. In contrast, about 20% of either single conditional KOs of $Grhl3^{Cre/+};Ezh2^{flox/flox}$ or compound cKOs of $Grhl3^{Cre/+};Ezh2^{flox/flox};Ezh1^{+/-}$ and $Grhl3^{Cre/+};Ezh2^{flox/flox};Ezh1^{-/-}$ embryos exhibited fully-open cleft palate (Figure 1e,f). The results also suggest that Ezh1 and Ezh2 have no synergetic roles in palatogenesis. We also found that these single or compound *Ezh2* cKO mutant embryos occasionally presented with digital hypoplasia (data not shown).

3.2 Cell proliferation is reduced in the palatal epithelium of conditional *Ezh2* mutant embryos

Histological staining of coronal sections at E14.5 consistently showed that the palatal shelves of epithelial *Ezh2* cKO mutants were not yet elevated even when the palatal shelves

of their wild-type or heterozygous littermates were elevated and had already begun to converge toward the midline (Figure 2a,b). While most embryos with this delayed elevation caught up and showed converged palate by E15.5, this was not always the case and complete elevation failure reflected the mechanism by which cleft palate was developed at a partial frequency.

To determine whether the palatal shelves of conditional *Ezh2* mutant embryos show defective cellular activities that may inhibit their ability to appropriately elevate, we performed immunofluorescent staining targeting markers of proliferation and apoptosis. Analysis of cleaved caspase 3 showed very low levels of apoptosis in the palate at E14.5, and there was no significant difference between wild-type and $Grhl3^{Cre/+};Ezh2^{flox/flox}$ mutants. We also performed immunofluorescent staining to detect Ki67 in mutant palatal shelves. No significant change was observed in the palatal mesenchyme of the mutants. However, the palatal epithelium showed reduced Ki67 expression at the middle and posterior regions of the palate, but there was no statistically significant change at the anterior palate of the mutants (Figure 2c–g).

3.3 Identification of cell types in the mouse embryo palates

To further understand the cellular mechanism that drives cleft palate formation with a loss of epithelial *Ezh2* function, scRNA-seq was performed to identify the transcriptional changes within the cells of mutant embryonic palate. The palatal shelves of $Grhl3^{Cre/+}$; $Ezh2^{flox/flox}$ mutant embryos and heterozygous control littermates were excised in the morning of E14 just prior to that key step of palatal elevation where the mutant phenotype becomes apparent. Tissues were dissociated to a single cell suspension and sequenced using the 10X Genomics 3’ Chromium method as we performed in a recent study (Gu et al., 2022). After quality control processing, we had transcriptome data for 10,518 control cells and 2,634 mutant cells. A Universal Manifold Approximation and Projection (UMAP) procedure was performed allowing the population structure of cells to be visualized in an unsupervised algorithm, where each dot represents a single cell base on its transcriptional identity (Becht et al., 2018). The distance between dots is proportional to the similarities between transcriptomes (Figure 3a). Cells were grouped into clusters representing distinct cell types and identified based on their highly conserved marker genes. The top three marker genes for each cluster are indicated (Figure 3a).

Ezh2 was conditionally removed from the palatal epithelium. Given the essential role of epithelial-mesenchymal interaction in the palatal development, differentially expressed genes (DEGs) could be detected in both palatal epithelial and mesenchymal cells of the cKO embryos. However, no DEGs were identified in the mesenchymal cells based on our current analysis setting. The major changes were found in epithelial cells which might indicate the transcriptome changes induced by Ezh2 deficiency limited to the epithelial cells at this specific timepoint (i.e., E14.0). However, it worths to further investigate on the transcriptome changes in both mesenchymal and epithelial cells at a serial timepoints. The mesenchymal cells uniquely expressed key markers *Sfrp*, *Col1a1*, and *Twist1*, which differentiate them from the rest of the cells. Four major epithelial clusters were differentiated at the resolution picked up by CellfindR (Yu et al., 2019). They were identified by top

markers *Krt14* (cluster 1.0; basal epithelium), *Sox2* (cluster 1.1; basal epithelium), *Sox21* (cluster 1.2; basal epithelium), and *Prr15l* (cluster 1.3; periderm). We identified one cluster of glial cells expressing *Fabp7* and *Foxd3*, and one small cluster of cells expressing possible markers of neuronal identity, including *Hand2* and *Snap25*. There were also two populations of endothelial cells and two populations of myeloid-lineage cells, as well as two groups of myogenic cells (Figure 3a). To explore the cell-cell communications through signaling pathways during palatogenesis, we performed CellChat (Ji et al., 2020) which showed that palatal mesenchymal cells had most ligand-receptor pairs and connections with the epithelial and endothelial as well as glial lineage cells (Figure 3b).

From our single-cell data we found that while *Ezh2* was expressed at relatively strong levels in the four epithelial populations, cells with appreciable *Ezh1* expression were minimal (Figure 3c,d). We then performed a pseudotime analysis of the epithelial cells across the entire dataset to map the trajectory of the represented cells. We found that the epithelial cells progressed from a more basic identity and split along two lineages. Additionally, the pseudotime map showed about four general cell identities, roughly corresponding to the four cell clusters separated during the initial analysis. Since immunostaining experiments suggested reduced Ki67 expression in the palatal epithelium of *Ezh2* cKO mutants, we also looked at *Mki67* in the single-cell dataset. We generated a feature map of epithelial cells expressing *Mki67* along the trajectory of the pseudotime analysis and found that most of the epithelial cells expressing *Mki67* are concentrated toward the basic end. Cells at the later stages of progression no longer express high levels of *Mki67*, reflecting a cell cycle exit as these cells begin to differentiate (Figure 4a). When comparing Mki67 transcript levels in the mutant and control groups, we found that all four epithelial clusters in the conditional *Ezh2* mutants showed cells with lower *Mki67* levels than those of controls, but only subcluster 1.2 showed statistical significance (Figure 4b,c). We validated *Mki67* expression by RT-qPCR using total RNA samples extracted from the whole palatal shelves, which showed a diminished level in the mutants, but there was no statistical significance (Figure 4d).

3.4 Altered transcripts of cell cycle regulators in the palatal epithelium of Ezh2 cKO mutant embryos

We further examined DEGs of the palatal shelf clusters identified through the scRNA-seq analysis. After Bonferroni correction, few genes remained statistically significant within each of the epithelial subpopulations. However, in cluster 1.2, approximately a dozen genes associated with cell cycle regulation are dysregulated, most of which were downregulated, in line with our findings that Ki67 or *Mki67* levels were reduced in the epithelium of *Ezh2* mutant palate. Among the top DEGs were the topoisomerase gene *Top2a* and the centromere protein encoding *Cenpf*. Both are key promotors of cell division, and both had reduced transcript levels in *Ezh2* cKO mutants (Figure 5a–h). RT-qPCR results using total RNA samples extracted from the whole palatal shelves showed diminished levels of both *Top2a* and *Cenpf* in the mutants, but there was no statistical significance (Figure 5d,h). Intriguingly, a top upregulated gene in the mutant cluster 1.2 is *Cdkn1a* that encodes p21, a key Cdk inhibitor and negative regulator of cell cycle progression (Figure 5i–k).

Since we recognized that there was extensive signaling predicted between all of the palatal cell populations, we considered a potential dysregulation in the mesenchyme as well due to epithelial-mesenchymal interactions. We resubclustered the mesenchyme separately and identified the major groups of cells (Figure S1a). We then compared the mesenchymal populations in mutant and control datasets, which did not reveal strong dysregulation of cell cycle regulators (Figure S1b–d), suggesting that epithelial *Ezh2* most likely only contributes to proliferation in the epithelium itself.

We also looked for expression of *Cdkn2a*, a target directly repressed by *Ezh2* which may provide insight into the mechanism by which *Ezh2* contributes to *Cdkn1a* expression and found there are few epithelial cells expressing appreciable levels of *Cdkn2a*, suggesting *Cdkn1a* may instead be a key target and means by which *Ezh2* controls proliferation in the palatal epithelium (Figure S2).

4 DISCUSSION

The dynamic morphological process of palatal development is manipulated by a complicated network which is highly coordinated between multiple molecular pathways. Accumulating evidence indicate a critical role of epigenome in influencing this complicated network. Our study demonstrated that ablation of *Ezh2* in mouse embryonic ectoderm caused partially penetrant cleft palate, associated with decreased proliferation of the palatal epithelial cells, particularly toward the posterior.

Although Ezh1 is dispensible for mouse survival, it has been shown that Ezh1 plays a synergistic role with Ezh2 in postnatal skin homeostasis in mice (Ezhkova et al., 2011). One notable finding we uncovered was that while penetrance was relatively low in our cKO mutants, it did not seem to be affected by any level of *Ezh1* insufficiency. Even though many of our experiments were performed with compound mutants with loss of *Ezh1* function or haploinsufficiency, penetrance of cleft palate was still around 20%. As such, *Ezh2* and PRC2 is likely to be solely responsible for the alterations in function of palatal epithelium.

In addition to the reduced proliferation as we found through immunofluorescent assay, scRNA-seq demonstrated a decreased expression of *Mki67* in the mutant group, further strengthening the link with *Ezh2* and cell cycle progression in the palatal shelf epithelia. Additionally, we were able to demonstrate a trajectory of differentiation through the generation of a pseudotime map. Through this we were able to show that cell cycle exit occurs early on by *Mki67* transcripts only within the least progressed cells, while the other groups do not express *Mki67*.

We found that while significantly dysregulated genes in *Ezh2* cKO mutant palate were minimal in most epithelial clusters, the subcluster 1.2 showed several top DEGs encoding factors involved in DNA replication or cell division. While many of the statistically significant DEGs were upregulated, reflecting the role of Ezh2 and the PRC as a transcriptional repression, most of the genes associated with proliferation were downregulated in cluster 1.2 of the mutant palate. One notable exception was *Cdkn1a*, which encodes p21, a major regulator that halts progression of the cell cycle and induces

senescence (Muñoz-Espín et al., 2013), which was upregulated in the *Ezh2* mutants. Since we also showed that proliferation was reduced in the epithelium of mutants at the middle and posterior regions, these are promising findings to strengthen the evidence for this role. As such we suggest that through *Ezh2*, PRC repression of cell cycle inhibitors, including *Cdn1a*, maintains proliferation of palatal epithelial cells, and that in its absence, cell cycle progression is reduced. Notably, the related *Cdkn2a* which is a known *Ezh2* target is not found at significant levels, suggesting *Cdkn1a* may be a main factor linking Ezh2 and proliferation in the palatal epithelium with a role similar to that which *Cdkn2a* plays in other tissues. Future studies will seek to clarify the regulatory methods by which *Ezh2* controls *Cdkn1a* and the altered proliferation markers in our model.

One remaining question is of the mechanism by which loss of epithelial *Ezh2* and reduced proliferation causes cleft palate. Increased proliferation in palate epithelium, or a failure of medial edge cells to exit the cell cycle, has been shown to be able to cause cleft palate. Alternatively, reduced proliferation in the mesenchyme may lead to hypomorphic palatal shelves that fail to converge, though it is unclear how reduced epithelial proliferation prevents palatogenesis. Palatal elevation is a delicate process and slight perturbations in the mechanical forces between oral structures can inhibit their ability to complete. Even the individuals of this model that do not show cleft palate, do show delayed elevation, occasionally resulting in elevation failure. The altered epithelium may just affect the shelves' ability to move just enough that sometimes they can recover with increased room above the tongue as development proceeds, but not always. One possibility may be that reduced proliferation results in a gap in the size of the pools of cells between the mutants and controls, that widens over the course of palatogenesis, leading to a significantly hypoplastic epithelium at the point of elevation, counteracting the mechanical forces from the mandible and within the palatal mesenchyme. Alternatively, this may reflect premature cell cycle exit and cellular differentiation, which could disrupt the epithelial-mesenchymal signaling interactions that are integral to palatogenesis, leading to a retarded ability to elevate. Future experimentation will help to clarify the relationship between sustained epithelial proliferation and palatal elevation that is regulated by *Ezh2* and lost in its absence.

Supplementary Material

Refer to Web version on PubMed Central for supplementary material.

Acknowledgments

We thank Elena Ezhkova of Icahn School of Medicine at Mount Sinai for sharing Ezh1 and Ezh2 mice; Mohammad Islam, Yu Ji, Arjun Stokes, Renato Reyes, Yutong Ji, and other related former Zhou lab members for their technical assistance or discussion; Bridget McLaughlin and Jonathan van Dyke of the UC Davis Flow Cytometry Shared Resource Center for their assistance with cell sorting; Diana Burkhart-Waco of the UC Davis DNA Technologies Core for help with single-cell RNA sequencing preparation. This study is supported by NIH (R01DE026737 & R01NS102261 to C.J.Z.) and the Shriners Hospitals for Children (71039 to B.S. and 85105 to C.J.Z.)

Data availability.

Single-cell RNA-seq data will be deposited to Gene Expression Omnibus at NIH after full analyses for different purposes.

REFERENCES

Adam M, Potter AS, Potter SS, 2017. Psychrophilic proteases dramatically reduce single-cell RNA-seq artifacts: a molecular atlas of kidney development. Development 144, 3625–3632. 10.1242/dev.151142 [PubMed: 28851704]

Aloia L, Di Stefano B, Di Croce L, 2013. Polycomb complexes in stem cells and embryonic development. Development 140, 2525–2534. 10.1242/dev.091553 [PubMed: 23715546]

Alvizi L, Ke X, Brito LA, Seselgyte R, Moore GE, Stanier P, Passos-Bueno MR, 2017. Differential methylation is associated with non-syndromic cleft lip and palate and contributes to penetrance effects. Scientific Reports 7, 2441. 10.1038/s41598-017-02721-0 [PubMed: 28550290]

Beaty TH, Murray JC, Marazita ML, Munger RG, Ruczinski I, Hetmanski JB, Liang KY, Wu T, Murray T, Fallin MD, Redett RA, Raymond G, Schwender H, Jin S-C, Cooper ME, Dunnwald M, Mansilla MA, Leslie E, Bullard S, Lidral AC, Moreno LM, Menezes R, Vieira AR, Petrin A, Wilcox AJ, Lie RT, Jabs EW, Wu-Chou YH, Chen PK, Wang H, Ye X, Huang S, Yeow V, Chong SS, Jee SH, Shi B, Christensen K, Melbye M, Doheny KF, Pugh EW, Ling H, Castilla EE, Czeizel AE, Ma L, Field LL, Brody L, Pangilinan F, Mills JL, Molloy AM, Kirke PN, Scott JM, Arcos-Burgos M, Scott AF, 2010. A genome-wide association study of cleft lip with and without cleft palate identifies risk variants near MAFB and ABCA4. Nat Genet 42, 525–529. 10.1038/ng.580 [PubMed: 20436469]

Beaty TH, Ruczinski I, Murray JC, Marazita ML, Munger RG, Hetmanski JB, Murray T, Redett RJ, Fallin MD, Liang KY, Wu T, Patel PJ, Jin S-C, Zhang TX, Schwender H, Wu-Chou YH, Chen PK, Chong SS, Cheah F, Yeow V, Ye X, Wang H, Huang S, Jabs EW, Shi B, Wilcox AJ, Lie RT, Jee SH, Christensen K, Doheny KF, Pugh EW, Ling H, Scott AF, 2011. Evidence for gene-environment interaction in a genome wide study of nonsyndromic cleft palate. Genetic Epidemiology 35, 469–478. 10.1002/gepi.20595 [PubMed: 21618603]

Becht E, McInnes L, Healy J, Dutertre CA, Kwok IWH, Ng LG, Ginhoux F, 2018. Dimentionality reduction for visualizing single-cell data using UMAP. Nature Biotechnology 37, 38–44

Béguelin W, Rivas MA, Calvo Fernández MT, Teater M, Purwada A, Redmond D, Shen H, Challman MF, Elemento O, Singh A, Melnick AM, 2017. EZH2 enables germinal centre formation through epigenetic silencing of CDKN1A and an Rb-E2F1 feedback loop. Nature Communications 8, 877. 10.1038/s41467-017-01029-x

Birnbaum S, Ludwig KU, Reutter H, Herms S, Steffens M, Rubini M, Baluardo C, Ferrian M, Almeida de Assis N, Alblas MA, Barth S, Freudenberg J, Lauster C, Schmidt G, Scheer M, Braumann B, Bergé SJ, Reich RH, Schiefke F, Hemprich A, Pötzsch S, Steegers-Theunissen RP, Pötzsch B, Moebus S, Horsthemke B, Kramer F-J, Wienker TF, Mossey PA, Propping P, Cichon S, Hoffmann P, Knapp M, Nöthen MM, Mangold E, 2009. Key susceptibility locus for nonsyndromic cleft lip with or without cleft palate on chromosome 8q24. Nature Genetics 41, 473–477. 10.1038/ng.333 [PubMed: 19270707]

Bjork BC, Turbe-Doan A, Prysak M, Herron BJ, Beier DR, 2010. Prdm16 is required for normal palatogenesis in mice. Human Molecular Genetics 19, 774–789. 10.1093/hmg/ddp543 [PubMed: 20007998]

Branch S, Chernoff N, Brownie C, Francis BM, 1999. 5-AZA-2'-deoxycytidine-induced dysmorphogenesis in the rat. Teratog Carcinog Mutagen 19, 329–338. [PubMed: 10495450]

Bulut HE, Ozdemir O, Başimoglu-Koca Y, Korkmaz M, Atalay A, 1999. Effects of a DNA demethylating agent--5-azacytidine--on testicular morphology during mouse embryo development. Okajimas Folia Anat Jpn 76, 47–53. 10.2535/ofaj1936.76.1_47 [PubMed: 10409845]

Burdi AR, Faist K, 1967. Morphogenesis of the palate in normal human embryos with special emphasis on the mechanisms involved. American Journal of Anatomy 120, 149–159. 10.1002/aja.1001200112

Bush JO, Jiang R, 2012. Palatogenesis: morphogenetic and molecular mechanisms of secondary palate development. Development 139, 231–243. 10.1242/dev.067082 [PubMed: 22186724]

Butali A, Suzuki S, Cooper ME, Mansilla AM, Cuenco K, Leslie EJ, Suzuki Y, Niimi T, Yamamoto M, Ayanga G, Erkhembaatar T, Furukawa H, Fujiwawa K, Imura H, Petrin AL, Natsume N, Beaty TH, Marazita ML, Murray JC, 2013. Replication of genome wide association identified candidate genes confirm the role of common and rare variants in PAX7 and VAX1 in the etiology

of nonsyndromic CL(P). Am J Med Genet A 161A, 965–972. 10.1002/ajmg.a.35749 [PubMed: 23463464]

Camerer E, Barker A, Duong DN, Ganesan R, Kataoka H, Cornelissen I, Darragh MR, Hussain A, Zheng Y-W, Srinivasan Y, Brown C, Xu S-M, Regard JB, Lin C-Y, Craik CS, Kirchhofer D, Coughlin SR, 2010. Local Protease Signaling Contributes to Neural Tube Closure in the Mouse Embryo. Developmental Cell 18, 25–38. 10.1016/j.devcel.2009.11.014 [PubMed: 20152175]

Campos Neves A.T. de S., Volpato LER, Espinosa MM, Aranha AMF, Borges AH, 2016. Environmental factors related to the occurrence of oral clefts in a Brazilian subpopulation. Niger Med J 57, 167–172. 10.4103/0300-1652.184064 [PubMed: 27397957]

Cannoodt R, Saelens W, Deconinck L, Saeys Y, 2021. Spearheading future omics analyses using dyngen, a multi-modal simulator of single cells. Nature Communications 12, 3942

Carette MJ, Ferguson MW, 1992. The fate of medial edge epithelial cells during palatal fusion in vitro: an analysis by DiI labelling and confocal microscopy. Development 114, 379–388. 10.1242/dev.114.2.379 [PubMed: 1591998]

Cuervo R, Valencia C, Chandraratna RAS, Covarrubias L, 2002. Programmed Cell Death Is Required for Palate Shelf Fusion and Is Regulated by Retinoic Acid. Developmental Biology 245, 145–156. 10.1006/dbio.2002.0620 [PubMed: 11969262]

Czeizel AE, Tímár L, Sárközi A, 1999. Dose-dependent Effect of Folic Acid on the Prevention of Orofacial Clefts. Pediatrics 104, e66–e66. 10.1542/peds.104.6.e66 [PubMed: 10586000]

Dixon MJ, Marazita ML, Beaty TH, Murray JC, 2011. Cleft lip and palate: understanding genetic and environmental influences. Nature Reviews Genetics 12, 167–178. 10.1038/nrg2933

Ezhkova E, Lien W-H, Stokes N, Pasolli HA, Silva JM, & Fuchs E (2011). EZH1 and EZH2 cogovern histone H3K27 trimethylation and are essential for hair follicle homeostasis and wound repair. Genes & Development, 25(5), 485–498. 10.1101/gad.2019811 [PubMed: 21317239]

Fan T, Jiang S, Chung N, Alikhan A, Ni C, Lee C-CR, Hornyak TJ, 2011. EZH2-Dependent Suppression of a Cellular Senescence Phenotype in Melanoma Cells by Inhibition of p21/CDKN1A Expression. Molecular Cancer Research 9, 418–429. 10.1158/1541-7786.MCR-10-0511 [PubMed: 21383005]

Garland MA, Reynolds K, Zhou CJ 2020a. Environmental mechanisms of orofacial clefts. Birth Defects Research 112, 1660–1698 [PubMed: 33125192]

Garland MA, Sun B, Zhang S, Reynolds K, Ji Y, Zhou CJ, 2020b. Role of epigenetics and miRNAs in orofacial clefts. Birth Defects Research 112, 1635–1659. 10.1002/bdr2.1802 [PubMed: 32926553]

Gonseth S, Shaw GM, Roy R, Segal MR, Asrani K, Rine J, Wiemels J, Marini NJ, 2019. Epigenomic profiling of newborns with isolated orofacial clefts reveals widespread DNA methylation changes and implicates metastable epiallele regions in disease risk. Epigenetics 14, 198–213. 10.1080/15592294.2019.1581591 [PubMed: 30870065]

Gu R, Zhang S, Saha SK, Ji Y, Reynolds K, McMahon M, Sun B, Islam M, Trainor PA, Chen Y, Xu Y, Chai Y, Burkart-Waco D, & Zhou CJ 2022. Single-cell transcriptomic signature and gene regulatory networks modulated by Wls in mammalian midline facial formation and clefts. Development 149, dev200533. [PubMed: 35781558]

Hannibal MC, Buckingham KJ, Ng SB, Ming JE, Beck AE, McMillin MJ, Gildersleeve HI, Bigham AW, Tabor HK, Mefford HC, Cook J, Yoshiura K, Matsumoto T, Matsumoto N, Miyake N, Tonoki H, Naritomi K, Kaname T, Nagai T, Ohashi H, Kurosawa K, Hou J-W, Ohta T, Liang D, Sudo A, Morris CA, Banka S, Black GC, Clayton-Smith J, Nickerson DA, Zackai EH, Shaikh TH, Donnai D, Niikawa N, Shendure J, Bamshad MJ, 2011. Spectrum of MLL2 (ALR) mutations in 110 cases of Kabuki syndrome. Am J Med Genet A 155A, 1511–1516. 10.1002/ajmg.a.34074 [PubMed: 21671394]

Howe LJ, Richardson TG, Arathimos R, Alvizi L, Passos-Bueno MR, Stanier P, Nohr E, Ludwig KU, Mangold E, Knapp M, Stergiakouli E, Pourcain BS, Smith GD, Sandy J, Relton CL, Lewis SJ, Hemani G, Sharp GC, 2019. Evidence for DNA methylation mediating genetic liability to non-syndromic cleft lip/palate. Epigenomics 11, 133–145. 10.2217/epi-2018-0091 [PubMed: 30638414]

Huang X-J, Wang X, Ma X, Sun S-C, Zhou X, Zhu C, Liu H, 2014. EZH2 is essential for development of mouse preimplantation embryos. Reprod. Fertil. Dev. 26, 1166–1175. [PubMed: 24153105]

Jin J-Z, Ding J, 2006. Analysis of cell migration, transdifferentiation and apoptosis during mouse secondary palate fusion. Development 133, 3341–3347. 10.1242/dev.02520 [PubMed: 16887819]

Ji Y, Garland MA, Sun B, Zhang S, Reynolds K, McMahon M, Rajakumar R, Islam MS, Liu Y, Chen Y, & Zhou CJ (2020). Cellular and developmental basis of orofacial clefts. Birth Defects Research, 112, 1558–1587. [PubMed: 32725806]

Jing J, Feng J, Li J, Han X, He J, Ho T-V, Du J, Zhou X, Urata M, Chai Y, 2019. Antagonistic interaction between Ezh2 and Arid1a coordinates root patterning and development via Cdkn2a in mouse molars. eLife 8, e46426. 10.7554/eLife.46426 [PubMed: 31259687]

John RM, Rougeulle C, 2018. Developmental Epigenetics: Phenotype and the Flexible Epigenome. Frontiers in Cell and Developmental Biology 6. [PubMed: 29459892]

Kanherkar RR, Bhatia-Dey N, Csoka AB, 2014. Epigenetics across the human lifespan. Frontiers in Cell and Developmental Biology 2. [PubMed: 25364711]

Kim H, Langohr IM, Faisal M, McNulty M, Thorn C, Kim J, 2018. Ablation of Ezh2 in neural crest cells leads to aberrant enteric nervous system development in mice. PLOS ONE 13, e0203391. 10.1371/journal.pone.0203391 [PubMed: 30169530]

Kim S, Lewis AE, Singh V, Ma X, Adelstein R, Bush JO, 2015. Convergence and extrusion are required for normal fusion of the mammalian secondary palate. PLOS Biology 13, e1002122. [PubMed: 25848986]

Kuriyama M, Udagawa A, Yoshimoto S, Ichinose M, Sato K, Yamazaki K, Matsuno Y, Shiota K, Mori C, 2008. DNA Methylation Changes during Cleft Palate Formation Induced by Retinoic Acid in Mice. The Cleft Palate Craniofacial Journal 45, 545–551. 10.1597/07-134.1 [PubMed: 18788878]

Kuzmichev A, Nishioka K, Erdjument-Bromage H, Tempst P, Reinberg D, 2002. Histone methyltransferase activity associated with a human multiprotein complex containing the Enhancer of Zeste protein. Genes & Development 16, 2893–2905. 10.1101/gad.1035902 [PubMed: 12435631]

Leslie EJ, Carlson JC, Shaffer JR, Butali A, Buxó CJ, Castilla EE, Christensen K, Deleyiannis FWB, Leigh Field L, Hecht JT, Moreno L, Orioli IM, Padilla C, Vieira AR, Wehby GL, Feingold E, Weinberg SM, Murray JC, Beaty TH, Marazita ML, 2017. Genome-wide meta-analyses of nonsyndromic orofacial clefts identify novel associations between FOXE1 and all orofacial clefts, and TP63 and cleft lip with or without cleft palate. Hum Genet 136, 275–286. 10.1007/s00439-016-1754-7 [PubMed: 28054174]

Leslie Elizabeth J., Carlson JC, Shaffer JR, Feingold E, Wehby G, Laurie CA, Jain D, Laurie CC, Doheny KF, McHenry T, Resick J, Sanchez C, Jacobs J, Emanuele B, Vieira AR, Neiswanger K, Lidral AC, Valencia-Ramirez LC, Lopez-Palacio AM, Valencia DR, Arcos-Burgos M, Czeizel AE, Field LL, Padilla CD, Cutiongco-de la Paz EMC, Deleyiannis F, Christensen K, Munger RG, Lie RT, Wilcox A, Romitti PA, Castilla EE, Mereb JC, Poletta FA, Orioli IM, Carvalho FM, Hecht JT, Blanton SH, Buxó CJ, Butali A, Mossey PA, Adeyemo WL, James O, Braimah RO, Aregbesola BS, Eshete MA, Abate F, Koruyucu M, Seymen F, Ma L, de Salamanca JE, Weinberg SM, Moreno L, Murray JC, Marazita ML, 2016. A multi-ethnic genome-wide association study identifies novel loci for non-syndromic cleft lip with or without cleft palate on 2p24.2, 17q23 and 19q13. Hum Mol Genet 25, 2862–2872. 10.1093/hmg/ddw104 [PubMed: 27033726]

Leslie Elizabeth J, Liu H, Carlson JC, Shaffer JR, Feingold E, Wehby G, Laurie CA, Jain D, Laurie CC, Doheny KF, McHenry T, Resick J, Sanchez C, Jacobs J, Emanuele B, Vieira AR, Neiswanger K, Standley J, Czeizel AE, Deleyiannis F, Christensen K, Munger RG, Lie RT, Wilcox A, Romitti PA, Field LL, Padilla CD, Cutiongco-de la Paz EMC, Lidral AC, Valencia-Ramirez LC, Lopez-Palacio AM, Valencia DR, Arcos-Burgos M, Castilla EE, Mereb JC, Poletta FA, Orioli IM, Carvalho FM, Hecht JT, Blanton SH, Buxó CJ, Butali A, Mossey PA, Adeyemo WL, James O, Braimah RO, Aregbesola BS, Eshete MA, Deribew M, Koruyucu M, Seymen F, Ma L, de Salamanca JE, Weinberg SM, Moreno L, Cornell RA, Murray JC, Marazita ML, 2016. A Genome-wide Association Study of Nonsyndromic Cleft Palate Identifies an Etiologic Missense Variant in GRHL3. Am J Hum Genet 98, 744–754. 10.1016/j.ajhg.2016.02.014 [PubMed: 27018472]

Leslie EJ, Taub MA, Liu H, Steinberg KM, Koboldt DC, Zhang Q, Carlson JC, Hetmanski JB, Wang H, Larson DE, Fulton RS, Kousa YA, Fakhouri WD, Naji A, Ruczinski I, Begum F, Parker MM, Busch T, Standley J, Rigdon J, Hecht JT, Scott AF, Wehby GL, Christensen K, Czeizel AE, Deleyiannis FW-B, Schutte BC, Wilson RK, Cornell RA, Lidral AC, Weinstock GM, Beaty

TH, Marazita ML, Murray JC, 2015. Identification of Functional Variants for Cleft Lip with or without Cleft Palate in or near PAX7, FGFR2, and NOG by Targeted Sequencing of GWAS Loci. The American Journal of Human Genetics 96, 397–411. 10.1016/j.ajhg.2015.01.004 [PubMed: 25704602]

Lindgren AM, Hoyos T, Talkowski ME, Hanscom C, Blumenthal I, Chiang C, Ernst C, Pereira S, Ordulu Z, Clericuzio C, Drautz JM, Rosenfeld JA, Shaffer LG, Velsher L, Pynn T, Vermeesch J, Harris DJ, Gusella JF, Liao EC, Morton CC, 2013. Haploinsufficiency of KDM6A is associated with severe psychomotor retardation, global growth restriction, seizures and cleft palate. Human Genetics 132, 537–552. 10.1007/s00439-013-1263-x [PubMed: 23354975]

Ludwig KU, Ahmed ST, Böhmer AC, Sangani NB, Varghese S, Klamt J, Schuenke H, Gültepe P, Hofmann A, Rubini M, Aldhorae KA, Steegers-Theunissen RP, Rojas-Martinez A, Reiter R, Borck G, Knapp M, Nakatomi M, Graf D, Mangold E, Peters H, 2016. Meta-analysis Reveals Genome-Wide Significance at 15q13 for Nonsyndromic Clefting of Both the Lip and the Palate, and Functional Analyses Implicate GREM1 As a Plausible Causative Gene. PLOS Genetics 12, e1005914. 10.1371/journal.pgen.1005914 [PubMed: 26968009]

Ludwig KU, Mangold E, Herms S, Nowak S, Reutter H, Paul A, Becker J, Herberz R, AlChawa T, Nasser E, Böhmer AC, Mattheisen M, Alblas MA, Barth S, Kluck N, Lauster C, Braumann B, Reich RH, Hemprich A, Pötzsch S, Blaumeiser B, Daratsianos N, Kreusch T, Murray JC, Marazita ML, Ruczinski I, Scott AF, Beaty TH, Kramer F-J, Wienker TF, Steegers-Theunissen RP, Rubini M, Mossey PA, Hoffmann P, Lange C, Cichon S, Propping P, Knapp M, Nöthen MM, 2012. Genome-wide meta-analyses of nonsyndromic cleft lip with or without cleft palate identify six new risk loci. Nature Genetics 44, 968–971. 10.1038/ng.2360 [PubMed: 22863734]

Marazita ML, Lidral AC, Murray JC, Field LL, Maher BS, Goldstein McHenry T, Cooper ME, Govil M, Daack-Hirsch S, Riley B, Jugessur A, Felix T, Morene L, Mansilla MA, Vieira AR, Doheny K, Pugh E, Valencia-Ramirez C, Arcos-Burgos M, 2009. Genome scan, fine-mapping, and candidate gene analysis of non-syndromic cleft lip with or without cleft palate reveals phenotype-specific differences in linkage and association results. Hum Hered 68, 151–170. 10.1159/000224636 [PubMed: 19521098]

Marazita ML, Murray JC, Lidral AC, Arcos-Burgos M, Cooper ME, Goldstein T, Maher BS, Daack-Hirsch S, Schultz R, Mansilla MA, Field LL, Liu Y, Prescott N, Malcolm S, Winter R, Ray A, Moreno L, Valencia C, Neiswanger K, Wyszynski DF, Bailey-Wilson JE, Albacha-Hejazi H, Beaty TH, McIntosh I, Hetmanski JB, Tunçbilek G, Edwards M, Harkin L, Scott R, Roddick LG, 2004. Meta-analysis of 13 genome scans reveals multiple cleft lip/palate genes with novel loci on 9q21 and 2q32-35. Am J Hum Genet 75, 161–173. 10.1086/422475 [PubMed: 15185170]

Moreno LM, Mansilla MA, Bullard SA, Cooper ME, Busch TD, Machida J, Johnson MK, Brauer D, Krahn K, Daack-Hirsch S, L'Heureux J, Valencia-Ramirez C, Rivera D, López AM, Moreno MA, Hing A, Lammer EJ, Jones M, Christensen K, Lie RT, Jugessur A, Wilcox AJ, Chines P, Pugh E, Doheny K, Arcos-Burgos M, Marazita ML, Murray JC, Lidral AC, 2009. FOXE1 association with both isolated cleft lip with or without cleft palate, and isolated cleft palate. Human Molecular Genetics 18, 4879–4896. 10.1093/hmg/ddp444 [PubMed: 19779022]

Mori C, Nakamura N, Okamoto Y, Osawa M, Shiota K, 1994. Cytochemical identification of programmed cell death in the fusing fetal mouse palate by specific labelling of DNA fragmentation. Anatomy and Embryology 190, 21–28. 10.1007/BF00185843 [PubMed: 7527193]

Mukhopadhyay N, Feingold E, Moreno-Uribe L, Wehby G, Valencia-Ramirez LC, Muñeton CPR, Padilla C, Deleyiannis F, Christensen K, Poletta FA, Orioli IM, Hecht JT, Buxó CJ, Butali A, Adeyemo WL, Vieira AR, Shaffer JR, Murray JC, Weinberg SM, Leslie EJ, Marazita ML, 2021. Genome-Wide Association Study of Non-syndromic Orofacial Clefts in a Multiethnic Sample of Families and Controls Identifies Novel Regions. Frontiers in Cell and Developmental Biology 9.

Mukhopadhyay N, Feingold E, Moreno-Uribe L, Wehby G, Valencia-Ramirez LC, Restrepo Muñeton CP, Padilla C, Deleyiannis F, Christensen K, Poletta FA, Orioli IM, Hecht JT, Buxó CJ, Butali A, Adeyemo WL, Vieira AR, Shaffer JR, Murray JC, Weinberg SM, Leslie EJ, Marazita ML, 2022. Genome-wide association study of multiethnic nonsyndromic orofacial cleft families identifies novel loci specific to family and phenotypic subtypes. Genet Epidemiol 46, 182–198. 10.1002/gepi.22447 [PubMed: 35191549]

Müller J, Hart CM, Francis NJ, Vargas ML, Sengupta A, Wild B, Miller EL, O'Connor MB, Kingston RE, Simon JA, 2002. Histone Methyltransferase Activity of a Drosophila Polycomb Group Repressor Complex. Cell 111, 197–208. 10.1016/S0092-8674(02)00976-5 [PubMed: 12408864]

Muñoz-Espín D, Cañamero M, Maraver A, Gómez-López G, Contreras J, Murillo-Cuesta S, Rodríguez-Baeza A, Varela-Nieto I, Ruberte J, Collado M, Serrano M, 2013. Programmed Cell Senescence during Mammalian Embryonic Development. Cell 155, 1104–1118. 10.1016/j.cell.2013.10.019 [PubMed: 24238962]

Muzumdar MD, Tasic B, Miyamichi K, Li L, Luo L, 2007. A global double-fluorescent Cre reporter mouse. genesis 45, 593–605. 10.1002/dvg.20335 [PubMed: 17868096]

O'Carroll D, Erhardt S, Pagani M, Barton SC, Surani MA, Jenuwein T, 2001. The Polycomb-Group GeneEzh2 Is Required for Early Mouse Development. Molecular and Cellular Biology 21, 4330–4336. 10.1128/MCB.21.13.4330-4336.2001 [PubMed: 11390661]

Reynolds K, Zhang S, Sun B, Garland MA, Ji Y, & Zhou CJ (2020). Genetics and signaling mechanisms of orofacial clefts. Birth Defects Research, 112, 1588–1634. [PubMed: 32666711]

Rogers JM, Francis BM, Sulik KK, Alles AJ, Massaro EJ, Zucker RM, Elstein KH, Rosen MB, Chernoff N, 1994. Cell death and cell cycle perturbation in the developmental toxicity of the demethylating agent, 5-Aza-2′-deoxycytidine. Teratology 50, 332–339. 10.1002/tera.1420500504 [PubMed: 7536356]

Satija R, Farrell JA, Gennert D, Schier AF, Regev A, 2015. Spatial reconstruction of single-cell gene expression data. Nature Biotechnology 33, 495–502

Schwarz D, Varum S, Zemke M, Schöler A, Baggiolini A, Draganova K, Koseki H, Schübeler D, Sommer L, 2014. Ezh2 is required for neural crest-derived cartilage and bone formation. Development 141, 867–877. 10.1242/dev.094342 [PubMed: 24496623]

Seelan RS, Mukhopadhyay P, Pisano MM, Greene RM, 2012. Developmental Epigenetics of the Murine Secondary Palate. ILAR Journal 53, 240–252. 10.1093/ilar.53.3-4.240 [PubMed: 23744964]

Shen X, Liu Y, Hsu Y-J, Fujiwara Y, Kim J, Mao X, Yuan G-C, Orkin SH, 2008. EZH1 Mediates Methylation on Histone H3 Lysine 27 and Complements EZH2 in Maintaining Stem Cell Identity and Executing Pluripotency. Molecular Cell 32, 491–502. 10.1016/j.molcel.2008.10.016 [PubMed: 19026780]

Shpargel KB, Mangini CL, Xie G, Ge K, Magnuson T, 2020. The KMT2D Kabuki syndrome histone methylase controls neural crest cell differentiation and facial morphology. Development 147, dev187997. 10.1242/dev.187997 [PubMed: 32541010]

Shpargel KB, Starmer J, Wang C, Ge K, Magnuson T, 2017. UTX-guided neural crest function underlies craniofacial features of Kabuki syndrome. Proceedings of the National Academy of Sciences 114, E9046–E9055. 10.1073/pnas.1705011114

Shu X, Shu S, Zhai Y, Zhu L, Ouyang Z, 2018. Genome-Wide DNA Methylation Profile of Gene cis-Acting Element Methylations in All-trans Retinoic Acid-Induced Mouse Cleft Palate. DNA and Cell Biology 37, 993–1002. 10.1089/dna.2018.4369

Shuler CF, Halpern DE, Guo Y, Sank AC, 1992. Medial edge epithelium fate traced by cell lineage analysis during epithelial-mesenchymal transformation in vivo. Developmental Biology 154, 318–330. 10.1016/0012-1606(92)90071-N [PubMed: 1385235]

Shull LC, Sen R, Menzel J, Goyama S, Kurokawa M, Artinger KB, 2020. The conserved and divergent roles of Prdm3 and Prdm16 in zebrafish and mouse craniofacial development. Developmental Biology 461, 132–144. 10.1016/j.ydbio.2020.02.006 [PubMed: 32044379]

Singh N, Gupta M, Trivedi CM, Singh MK, Li L, Epstein JA, 2013. Murine craniofacial development requires Hdac3-mediated repression of Msx gene expression. Developmental Biology 377, 333–344. 10.1016/j.ydbio.2013.03.008 [PubMed: 23506836]

Spilson S, Kim H, Chung K, 2001. Association between maternal diabetes mellitus and newborn oral cleft. Ann Plast Surg 47, 477–481. 10.1097/00000637-200111000-00001 [PubMed: 11716256]

Stuart T, Butler A, Hoffman P, Hafemeister C, Papalexi E, Mauck WM III, Hao Y, Stoeckius M, Smibert P, Satija R, 2019. Comprehensive Integration of Single-Cell Data. Cell 177, 1888–1902.e21. 10.1016/j.cell.2019.05.031 [PubMed: 31178118]

Sun Y, Huang Y, Yin A, Pan Y, Wang Y, Wang C, Du Y, Wang M, Lan F, Hu Z, Wang G, Jiang M, Ma Junqing, Zhang X, Ma H, Ma Jian, Zhang W, Huang Q, Zhou Z, Ma L, Li Y, Jiang H, Xie L, Jiang Y, Shi B, Cheng J, Shen H, Wang L, Yang Y, 2015. Genome-wide association study identifies a new susceptibility locus for cleft lip with or without a cleft palate. Nat Commun 6, 6414. 10.1038/ncomms7414 [PubMed: 25775280]

Teng T, Teng CS, Kaartinen V, & Bush JO (2022). A unique form of collective epithelial migration is crucial for tissue fusion in the secondary palate and can overcome loss of epithelial apoptosis. Development, 149(10). 10.1242/dev.200181

van Rooij IA, Ludwig KU, Welzenbach J, Ishorst N, Thonissen M, Galesloot TE, Ongkosuwito E, Bergé SJ, Aldhorae K, Rojas-Martinez A, Kiemeney LA, Vermeesch JR, Brunner H, Roeleveld N, Devriendt K, Dormaar T, Hens G, Knapp M, Carels C, Mangold E, 2019. Non-Syndromic Cleft Lip with or without Cleft Palate: Genome-Wide Association Study in Europeans Identifies a Suggestive Risk Locus at 16p12.1 and Supports SH3PXD2A as a Clefting Susceptibility Gene. Genes (Basel) 10. 10.3390/genes10121023 [PubMed: 31861950]

Voss AK, Vanyai HK, Collin C, Dixon MP, McLennan TJ, Sheikh BN, Scambler P, Thomas T, 2012. MOZ Regulates the Tbx1 Locus, and Moz Mutation Partially Phenocopies DiGeorge Syndrome. Developmental Cell 23, 652–663. 10.1016/j.devcel.2012.07.010 [PubMed: 22921202]

Watkins SE, Meyer RE, Strauss RP, Aylsworth AS, 2014. Classification, Epidemiology, and Genetics of Orofacial Clefts. Clinics in Plastic Surgery 41, 149–163. 10.1016/j.cps.2013.12.003 [PubMed: 24607185]

Xu J, Wang Z, Lu W, Jiang H, Lu J, Qiu J, Ye G, 2019. EZH2 promotes gastric cancer cells proliferation by repressing p21 expression. Pathology - Research and Practice 215, 152374. 10.1016/j.prp.2019.03.003 [PubMed: 30952377]

Xu Z, Lie RT, Wilcox AJ, Saugstad OD, Taylor JA, 2019. A comparison of DNA methylation in newborn blood samples from infants with and without orofacial clefts. Clinical Epigenetics 11, 40. 10.1186/s13148-019-0638-9 [PubMed: 30832715]

Yang S, Corbett SE, Koga Y, Wang Z, Johnson WE, Yajima M, Campbell JD, 2020. Decontamination of ambient RNA in single-cell RNA-seq with DecontX. Genome Biology 21, 57. 10.1186/s13059-020-1950-6 [PubMed: 32138770]

Yu KS, Frumm SM, Park JS, Lee K, Wong DM, Byrnes L, Knox SM, Sneddon JB, Tward AD, 2019. Development of the Mouse and Human Cochlea at Single Cell Resolution. bioRxiv 739680. 10.1101/739680

Yu Y, Zuo X, He M, Gao J, Fu Y, Qin C, Meng L, Wang W, Song Y, Cheng Y, Zhou F, Chen G, Zheng X, Wang X, Liang B, Zhu Z, Fu X, Sheng Y, Hao J, Liu Z, Yan H, Mangold E, Ruczinski I, Liu J, Marazita ML, Ludwig KU, Beaty TH, Zhang X, Sun L, Bian Z, 2017. Genome-wide analyses of non-syndromic cleft lip with palate identify 14 novel loci and genetic heterogeneity. Nature Communications 8, 14364. 10.1038/ncomms14364

Yuan X, Qiu L, Pu Y, Liu C, Zhang X, Wang C, Pu W, Fu Y, 2016. Histone acetylation is involved in TCDD-induced cleft palate formation in fetal mice. Mol Med Rep 14, 1139–1145. 10.3892/mmr.2016.5348 [PubMed: 27279340]

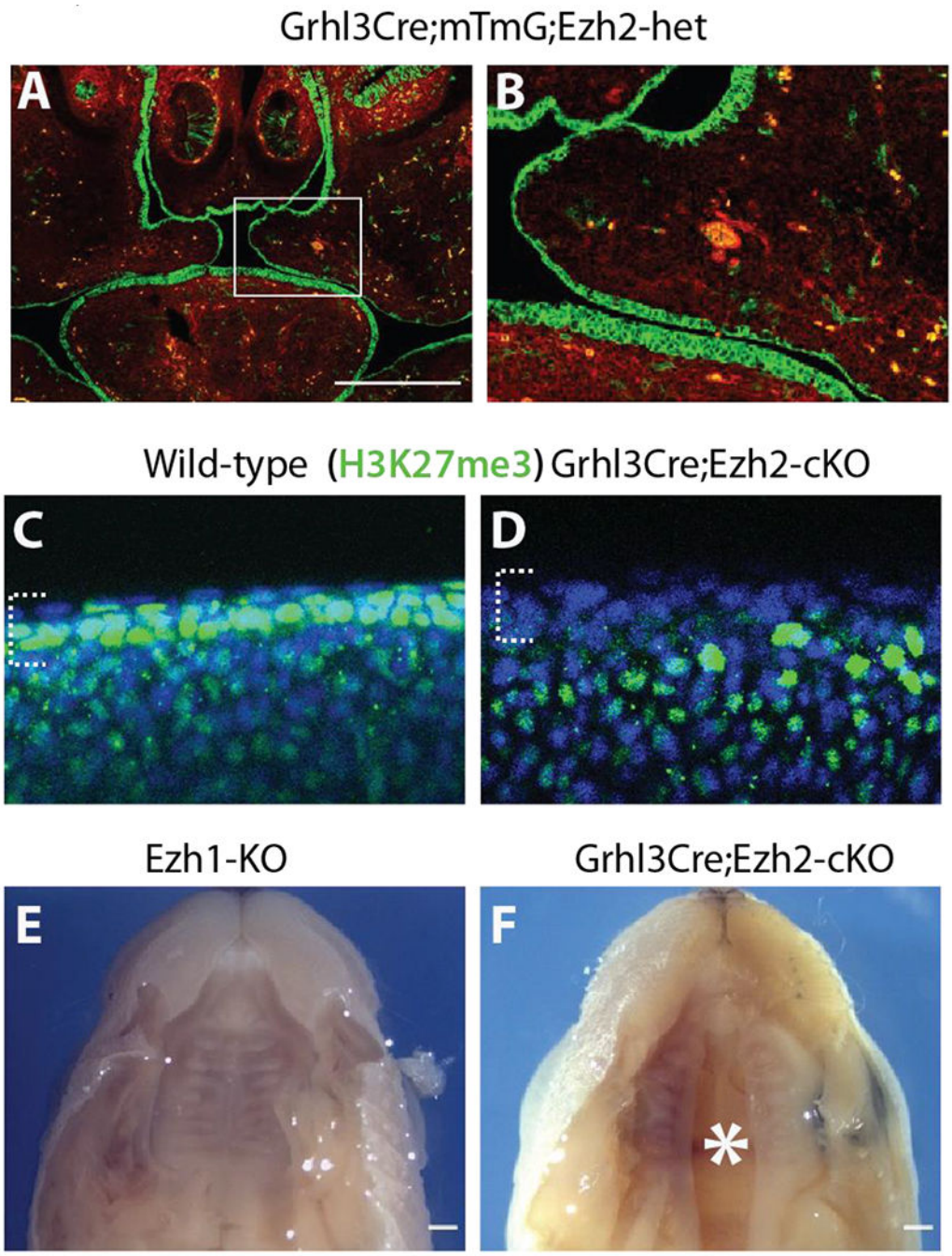

Figure 1. Conditional ablation of Ezh2 in palatal epithelia abolishes H3K27 trimethylation and causes cleft palate.

(A,B) Rosa26-mTmG fate-mapping shows Cre recombination in Grhl3-Cre^{+} oral ectoderm expressing eGFP at E14.5, while cell in which Cre was never activated express td-Tomato. Occasional small colonies of mesenchyme cells expressing eGFP are apparent in enlarged palatal shelf image (B enlarged from squared area in A). (C,D) H3K27me3 immunofluorescence shows strong staining in the medial edge epithelia (MEE, bracket in C) in the wild-type control palate, which is missing in the Grhl3Cre;Ezh2-cKO palatal MEE (dashed bracket in D) at E14.5. (E,F) Palate is fully closed in 100% Ezh1-KO embryos at

E18.5 (E), while palate remains open (white asterisk) in about 20% of Grhl3Cre;Ezh2-cKO with or without Ezh1 ablation at E18.5 (F). Scale bars = 500μm.

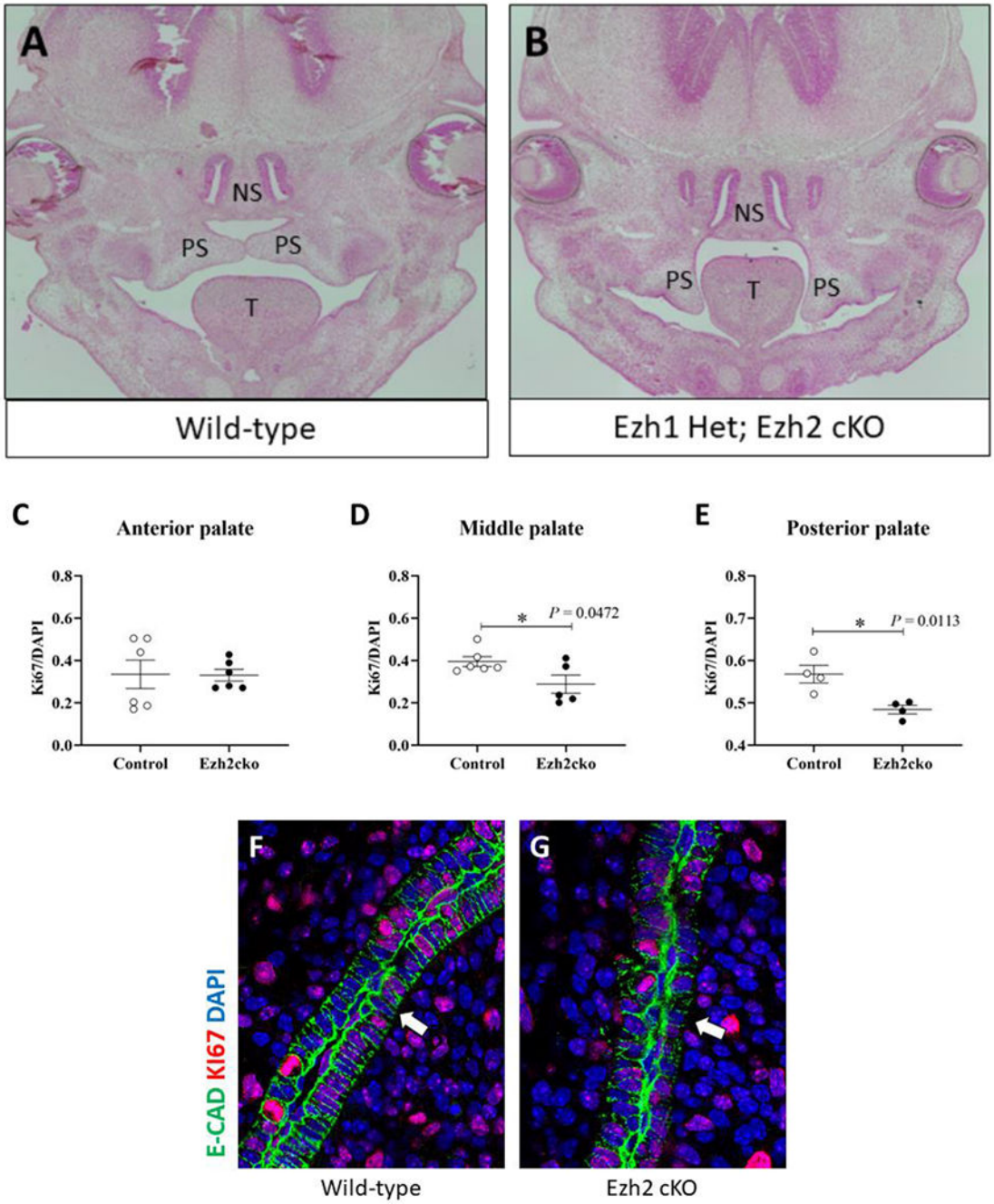

Figure 2. Altered function in palatal shelves of Ezh2 mutant embryos.

(A-B) Hematoxylin/Eosin stain of coronal sections of E14.5 embryos. Palatal shelves of wild-type control embryos lacking Cre (A) have elevated, while the palatal shelves of *Grhl3*$^{Cre/+}$; *Ezh2*$^{flox/flox}$ mutant littermates (B) are still vertical. NS = nasal septum, PS = palatal shelf, T = tongue. (C-F) Proliferation is reduced in the posterior palatal shelf epithelium of *Ezh2* mutant palate. Percentages of Ki67+ cells in the epithelium of control and Grhl3-Cre *Ezh2* cKO mutant palatal shelves quantified at the anterior (C), middle (D), and posterior (E) region. (F-G) Comparison of the Ki67 staining in the posterior palate

epithelium of control (F) and cKO mutant (G) embryo at E14.5. Ki67 is shown in red. E-cadherin is shown in green. DAPI is shown in blue.

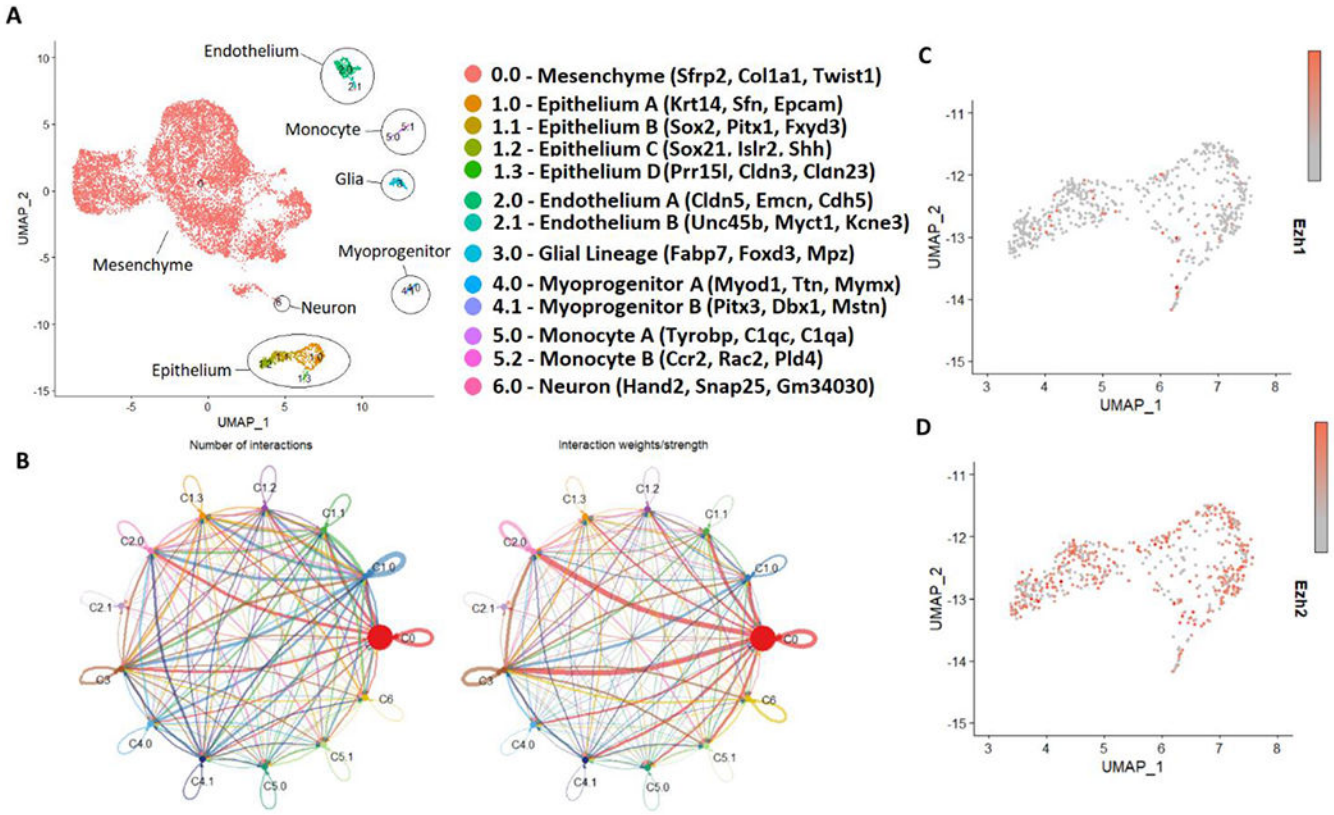

Figure 3. scRNA-seq reveals palatal cell features, cell-cell communications among different clusters, and Ezh1/Ezh2 expression in the palatal epithelium.

(A) UMAP showing representative relationships between E14.5 palatal shelf cells with top markers identifying each cluster. (B) CellChat diagram for signaling interactions between different cell clusters based on expressed pathway components. (C-D) Expression feature maps of *Ezh1* and *Ezh2* in the palate epithelial clusters in which they were ablated. *Ezh1* (C) expression is limited in the epithelium, while *Ezh2* (D) shows high expression in the epithelium.

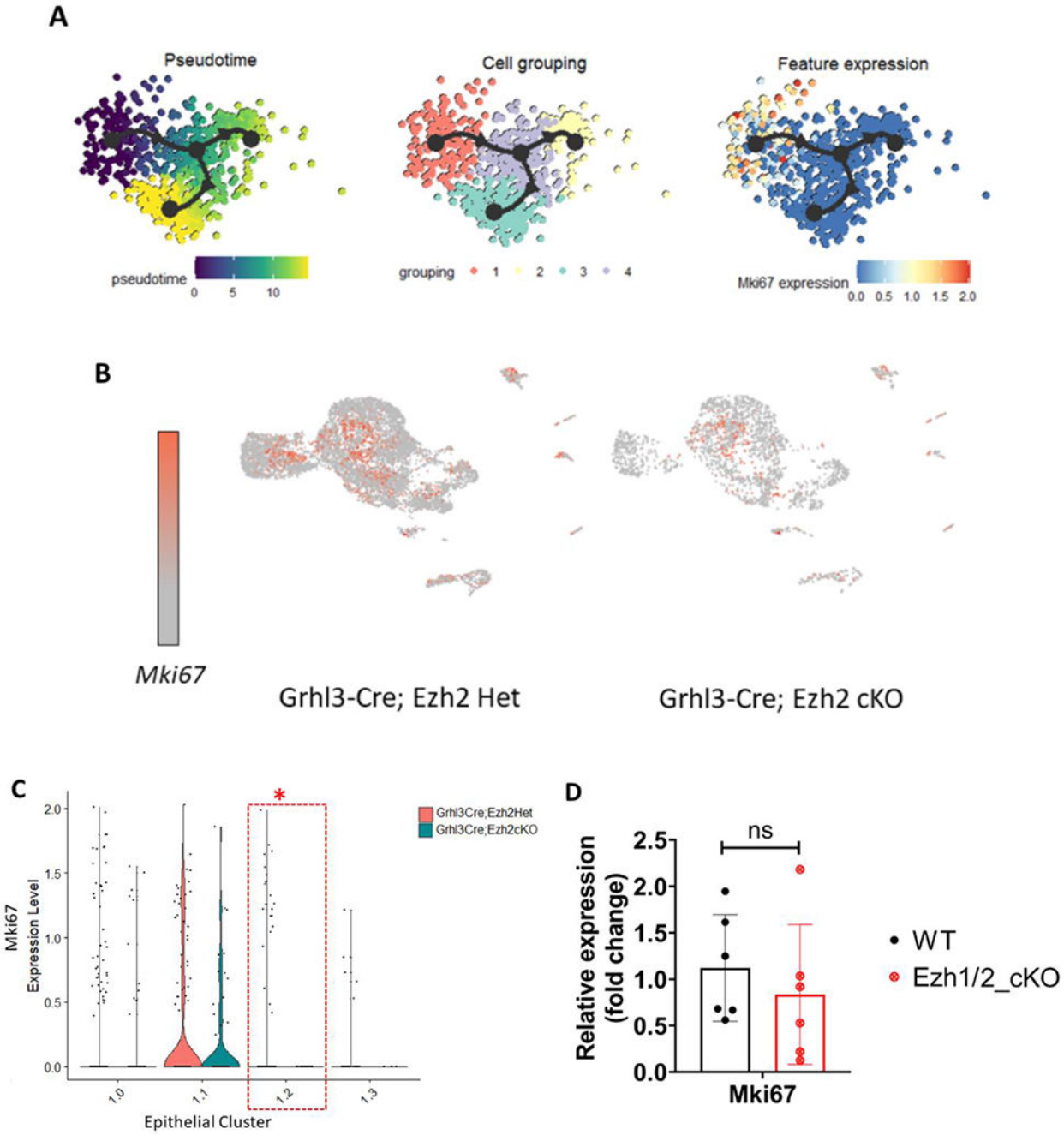

Figure 4. Developmental trajectory of palatal epithelium and diminished *Mki67* expression in a subcluster of mutant epithelium.

(A) Pseudo-time analysis of epithelial cells with arrows indicating differentiation split along two distinct trajectories, with cell clusters representing different points in differentiation *Mki67* expression indicates differentiation largely correlates with a reduction in proliferation (B-D) scRNAseq data reveals reduced expression of proliferation marker *Mki67* in palatal epithelium of *Ezh2* cKO mutant embryo. Expression map (B) showing cells with *Mki67* expression in heterozygous control and cKO mutant datasets. Violin plot (C) showing significant reduction of Mki67 transcript levels in the mutant epithelial subcluster 1.2 (*,

P<0.05). Real-time PCR results (D) demonstrate no significant (ns, P > 0.05) changes of *Mki67* in the whole palatal tissue between the mutants and littermate control groups.

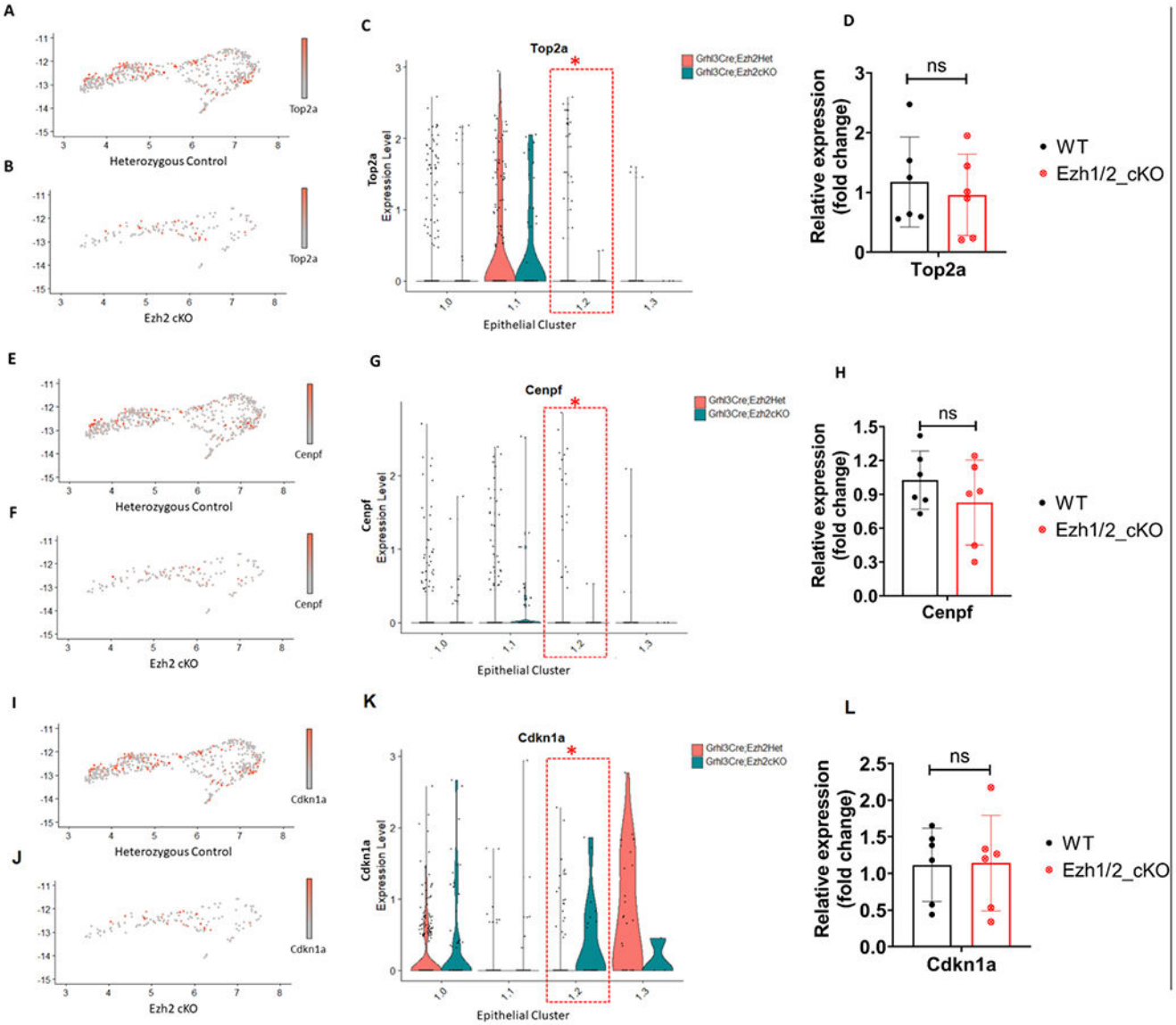

Figure 5. Cell cycle regulators are altered in Ezh2-cKO palate epithelium.

(A-D) *Top2a* transcripts are reduced in epithelial palate cells of Ezh2 mutant embryos. Feature maps showing *Top2a* expression in control (A) and mutant datasets (B). Violin plot showing significantly diminished *Top2a* expression in the mutant epithelial subcluster 1.2 (C). RT-qPCR showing no significant (ns, $P > 0.05$) changes of *TOP2a* expression in the whole palatal primordia (D). (E-H) *Cenpf* transcripts are significantly diminished in epithelial subcluster 1.2 of Ezh2 mutant embryos. (I-L) *Cdkn1a* transcripts are significantly increased in epithelial subcluster 1.2 of Ezh2 mutant embryos. *, $P < 0.05$.